

Flex-TPU: A Flexible TPU with Runtime Reconfigurable Dataflow Architecture

Mohammed Elbitty, Peyton Chandarana, and Ramtin Zand

Department of Computer Science and Engineering, University of South Carolina, Columbia, SC 29208, USA

e-mail: elbitty@ieee.org, psc@email.sc.edu, ramtin@cse.sc.edu

Abstract—Tensor processing units (TPUs) are one of the most well-known machine learning (ML) accelerators utilized at large scale in data centers as well as in tiny ML applications. TPUs offer several improvements and advantages over conventional ML accelerators, like graphical processing units (GPUs), being designed specifically to perform the multiply-accumulate (MAC) operations required in the matrix-matrix and matrix-vector multiplies extensively present throughout the execution of deep neural networks (DNNs). Such improvements include maximizing data reuse and minimizing data transfer by leveraging the temporal dataflow paradigms provided by the systolic array architecture. While this design provides a significant performance benefit, the current implementations are restricted to a single dataflow consisting of either input, output, or weight stationary architectures. This can limit the achievable performance of DNN inference and reduce the utilization of compute units. Therefore, the work herein consists of developing a reconfigurable dataflow TPU, called the Flex-TPU, which can dynamically change the dataflow per layer during run-time. Our experiments thoroughly test the viability of the Flex-TPU comparing it to conventional TPU designs across multiple well-known ML workloads. The results show that our Flex-TPU design achieves a significant performance increase of up to $2.75\times$ compared to conventional TPU, with only minor area and power overheads.

Index Terms—Tensor processing unit (TPU), AI hardware accelerator, machine learning, systolic array, ML architecture.

I. INTRODUCTION

In 2015, Google launched its tensor processing unit (TPU) project adopting the systolic array architecture, dating back to as early as 1979 [1], to accelerate machine learning (ML) workloads [2], [3]. The first version of Google’s TPU was primarily designed to accelerate ML workloads in large data centers utilizing 8-bit integer (INT8) multiply and accumulate (MAC) units to offer a peak performance of 92 tera operations per second (TOPS) [3]. The most recent version of the TPU, the TPU v4, can accelerate training and inference using the TPU’s internal 16-bit brain-float (BF16) and INT8 precisions to offer up to 275 teraflops of computational power [4]. In 2019, Google launched a smaller and low-power version of the TPU, called the Coral Edge TPU, that is suited to accelerate the inference of the ML workloads at the edge [5]–[8]. The Edge TPU uses INT8 MAC core units [9] and realizes a peak performance of four TOPS.

In contrast to the graphical processing units (GPUs) already employed for this task, TPUs were specifically designed to accelerate the common matrix-matrix and matrix-vector multiplications dominant in ML workloads with a particu-

lar focus on maximizing data reuse while minimizing data transfer. Since their advent in 2015, several variations of TPU have been proposed [4], [10]–[14], which similarly adopt the systolic array architecture but focus on modifying the microarchitecture to achieve improvements in performance, power, energy, etc. For example, in 2022 the APTPU [11] was proposed which leverages approximate multipliers and adders in the systolic array processing elements (PEs) to improve the performance, area, and power of the TPU design. Another example is UPTPU [12], which utilizes power-gating to reduce the energy consumption of the TPUs.

The typical systolic array architecture consists of an $N \times N$ array of PEs, each of which implements a MAC operation using a single multiplier and adder along with some registers to store data for reuse. The dataflow in the systolic array is a mapping scheme that depends on the microarchitecture of PEs and determines how the input data is fed to the array along with how the partial results and outputs are generated and stored. Instead of loading and storing to and from memory for each computation, each PE in the systolic array typically employs one of the following dataflow paradigms:

- **Input Stationary (IS):** The inputs (or activations) remain fixed in the systolic array PEs while the weights are distributed horizontally.
- **Output Stationary (OS):** Outputs are attached to MAC units as the inputs and weights are circulated among the units. As new inputs and weights are loaded and multiplied, they are then accumulated directly into the stationary outputs.
- **Weight Stationary (WS):** Each weight is pre-loaded into a register attached to the MAC within each PE. During each cycle, the input activation data is multiplied by the fixed weights and broadcast across the systolic array’s other processing elements.

Even in 2024, most of the TPUs used in larger data centers, or even the edge TPUs like the Google Coral Edge TPU [15], have only been engineered with one of these three dataflow architectures in hardware. However, this singular static dataflow architecture may not always provide the optimal performance depending on the specific implementation of a deep neural network’s (DNN) layers leading to significant performance limitations. As shown in Fig. 1, our simulations of the ResNet-18 [16] convolutional neural network (CNN), show that in many cases the many layers of a DNN can perform better

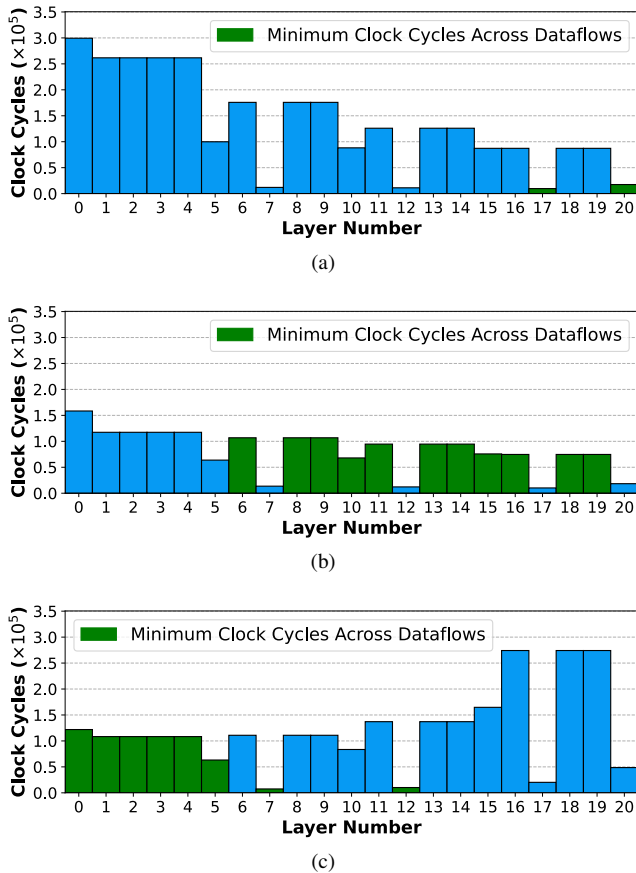


Fig. 1: Cycles required for executing each layer in ResNet-18 model using static dataflow architectures: (a) input stationary, (b) output Stationary, and (c) weight stationary. The layer-wise comparison shows that the optimal dataflow can be different in each layer of the network emphasizing the potential benefits of a flexible TPU with a run-time reconfigurable dataflow.

on a heterogenous distribution of dataflows. For example in Fig. 1, we see that ResNet-18’s first five layers are fastest on the weight stationary dataflow while the more intermediate and final layers perform optimally on the output and input stationary dataflows, respectively. As later shown in Fig. 5, a majority of the TPU’s area is consumed by the systolic array and accounts for 77%-80% of the entire TPU’s area consuming approximately 50%-89% of the overall power consumption of the architecture. Thus, modifying the microarchitecture of the systolic array to support multiple different dataflows could lead to significant performance speedups for the TPU as a whole.

In this paper, to increase the performance of the TPU, we propose a flexible runtime-reconfigurable dataflow TPU, called the Flex-TPU, in which the dataflow architecture of the systolic array can be reconfigured for each layer of the DNN according to the workload characteristic. Herein, our contributions consist of the following:

- A modified PE microarchitecture to support runtime-reconfigurable dataflows.
- The implementation of the modified processing elements

into a functional TPU.

- Thorough experimentation which shows the validity and increased performance of our design.

The remainder of the paper is organized as follows. In Section II we present our Flex-TPU architecture and discuss the specific changes we make to the PE microarchitecture. In Section III we discuss the performance gains resulting from the flexibility in dataflow in the Flex-TPU and the marginal overheads incurred over conventional TPUs. Finally, we conclude the paper in Section IV.

II. PROPOSED FLEX-TPU

The systolic array is the core element of any TPU architecture. A systolic array consists of two or multi-dimensional arrays of processing elements (PEs). Each PE in the systolic array implements a multiply-and-accumulate (MAC) operation by multiplying the weights and inputs with a multiplier and then adding this product with any previously computed partial sums using an accumulator. The result of this summation is then kept in the same PE or broadcast downstream to other PEs to be used in further computations. Regardless of the dataflow type, this MAC operation occurs in each PE of the systolic array to accomplish matrix-matrix or matrix-vector multiplication while maximizing data reuse without introducing additional data transfer overhead.

The primary distinction between different TPU architectures is typically the dataflow of the systolic array and its PEs. Each dataflow has its own advantages and trade-offs for ML workloads regarding power, data transfer, and compute units’ utilization efficiency dependent on specific workload characteristics. The choice between the IS, OS, or WS dataflow largely depends on the objectives of the computation, such as maximizing data reuse, minimizing memory bandwidth, or reducing latency. As shown in Fig. 1, ResNet-18’s optimal dataflow varies across the layers between all three dataflows. Hence, selecting the optimal dataflow at runtime for each layer can lead to significant performance gains.

Figure 2 shows the overall architecture of our proposed Flex-TPU, which is equipped with a runtime dataflow reconfigurability feature. Similar to a conventional TPU, our proposed Flex-TPU design consists of weight memory, input memory, output memory, and a systolic array of size $S = N \times N$ PEs surrounded by the first-in-first-out (FIFO) buffers as depicted in Fig. 2. Additionally, our Flex-TPU includes a *Weight/IFMap Register File* that stores the fixed or the “stationary” weights or the IFMaps - depending on the selected dataflow - with output ports distributed among the PEs in the systolic array. Moreover, the *Dataflow Generator* block generates the memory read/write addresses to store or retrieve the IFMaps, weights, and OFMap according to the selected dataflow dictated by the *Configuration Management Unit (CMU)*. The CMU selects the dataflow for each layer of the ML workload by informing the *Dataflow Generator* and by reconfiguring the PEs within the systolic array to work according to the pre-determined dataflow for each layer. It is worth mentioning that the dataflow of each layer of the

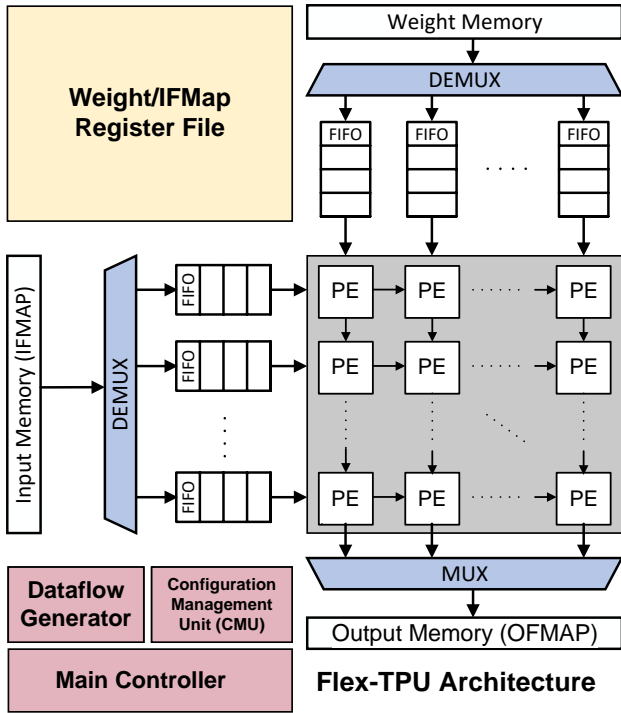


Fig. 2: The proposed Flex-TPU Architecture.

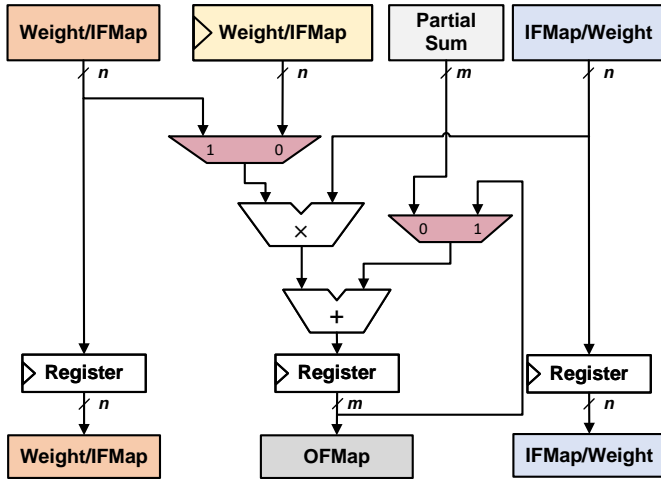


Fig. 3: The proposed Flex-TPU processing element (PE) with runtime reconfigurable dataflow.

ML model is determined after training and before deployment of the model on the Flex-TPU, reducing the complexity of the hardware. The *Main Controller* handles the data transfer between memories/FIFOs and the systolic array, programming the CMU units, and writes to the *Weight/IFMap Register File*. The proposed Flex-TPU’s architecture differs from that of the conventional TPU in two primary ways: 1) the processing elements within the systolic array and 2) the controller driving the dataflow selections.

Figure 3 shows the microarchitecture of a processing element in the Flex-TPU, which has one extra register and two

multiplexers (MUXs) compared to the PE of a conventional TPU. The MUXs are controlled by the configuration management unit and are utilized to select the optimal dataflow for each layer in the ML model during runtime. As investigated in Section III-B, adding these three extra components to each PE in the systolic array does moderately increase both area and power consumption, but the flexibility of the design provides a significant performance increase as discussed in section III-A.

As shown in Fig. 4, there are three possible runtime configurations of our flexible PEs that correspond to each of the three common dataflows: IS, OS, and WS. In Fig. 4 (a), the input stationary (IS) configuration is shown where the input-feature-map (IFMap) is fixed in a register in the PE. To accomplish the IS dataflow during runtime, the *CMU* sends both MUXs a “0” control signal and the *Main Controller* pins the IFMap in the register in the PE. The IS dataflow often excels for layers with small stridden convolutions or depthwise convolutions due to the high input reuse. By minimizing the movement of heavily reused input data, a significant amount of bandwidth can be saved, particularly in memory-bound operations or power-constrained environments.

Figure 4(b) shows the OS configuration mode of the PE. In this mode, the IFMaps and Weights are multiplied and then moved through the PEs in the systolic array to be reused in further operations. The partial sums remain fixed in the PEs and keep accumulating to form the final output feature map (OFMap) of the layer. The OS dataflow mode is triggered by a “1” control signal being sent from the *CMU* to the MUXs of each PE and thus leads to the output of the MAC being fixed inside of the accumulator. The OS dataflow is typically advantageous in deeper layers of DNNs where a large number of partial sums are being accumulated. Thus, keeping the output fixed within the PE minimizes the need for frequent memory stores of intermediate results benefiting layers with higher computational intensity per output.

Figure 4 (c) shows the runtime configuration for the weight stationary (WS) dataflow. The WS dataflow mode is activated with a “0” control signal sent from the *CMU*. However, instead of the IFMap being fixed in the added register in the PE, the weight is fixed for the duration of the computation. This can be advantageous in the first layers of DNNs where the ratio of input to weights is high. As a result, keeping the weights stationary yields the efficient use of memory bandwidth and improves the overall computational throughput.

Selecting the optimal dataflow strategy is dependent on multiple layer-specific characteristics such as IFMap dimensions, filter sizes, number of channels, and strides. To find the optimal dataflow strategy for each layer in the DNN, we should run each trained model on the Flex-TPU three times, once for each dataflow, during the development phase. From these three runs, the dataflow that executes each layer’s computation in the least number of clock cycles is then selected as the optimal dataflow for that layer. Following this one-time pre-deployment optimization procedure the optimal dataflow is then programmed into the *CMU* by the *Main Controller* and the *CMU* subsequently drives each processing element’s

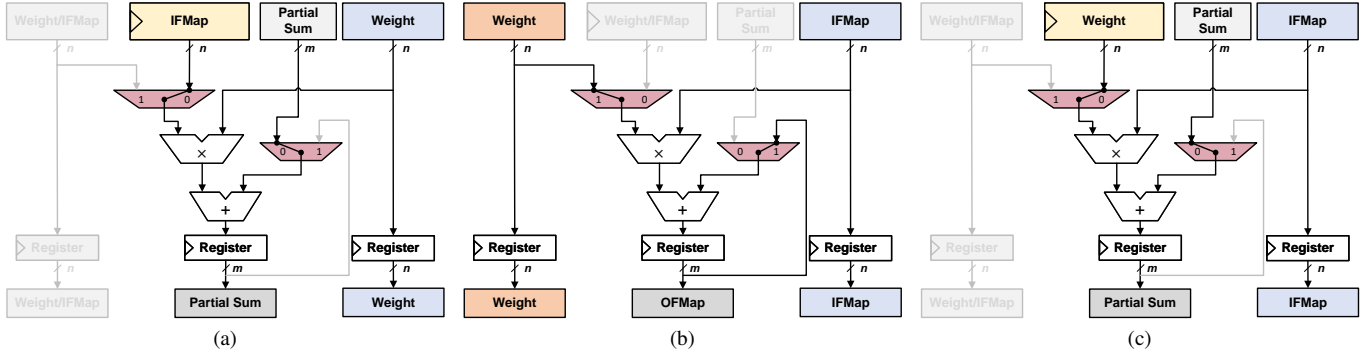


Fig. 4: The three flexible PE dataflow configurations controlled by the two added MUXs: (a) IS, (b) OS, and (c) WS modes.

MUXs to reconfigure them with the optimal dataflow during runtime as well as informing the *Dataflow Generator* to generate the read/write indices accordingly. This process only needs to be performed once per DNN model prior to deployment and during the development phase to optimize the per-layer dataflows. While not a part of this work, we plan to explore other methods of selecting the optimal dataflow for networks deployed on the Flex-TPU in the future.

III. RESULTS AND DISCUSSIONS

As mentioned in Section II, the proposed Flex-TPU design modifies the processing elements in the systolic array architecture to introduce dataflow flexibility with the inclusion of a single extra register and two multiplexers. While this work does not focus on making improvements to the other components of the architecture, like the FIFOs, the systolic array is estimated to utilize approximately 77% to 80% of the entire TPU’s area, as shown in Fig. 5. Additionally, the systolic array also accounts for approximately 50%-89% of the power consumption depending on the systolic array size S . Thus, modifying the PEs of the systolic array can significantly affect the overall performance of the TPU. The layout of the in-house implementation of a TPU chip is shown in Fig. 5 and demonstrates the overall ratio of the systolic array’s area compared to the entire layout.

Herein, our results in Section III-A show the benefits of the Flex-TPU architecture in providing layer-by-layer dataflow optimizations to increase the overall throughput and performance of a systolic array of size $S = 32 \times 32$. As mentioned before, while there are significant performance gains to the Flex-TPU design, this increased performance does contribute to a slight increase in area and power consumption that is discussed in Section III-B. The performance, power, and area results are obtained using ScaleSim V2 [17], [18], a cycle-accurate simulator for ML accelerators, and Synopsys Design Compiler along with the 45nm Nangate Open Cell Library.

A. Performance

In our experiments, the optimal dataflow was found by running each of the selected DNN models on the three different dataflows, IS, OS, and WS, using the ScaleSim V2 systolic

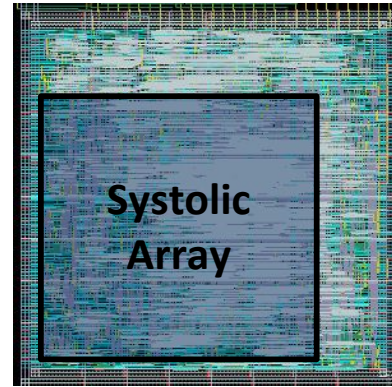


Fig. 5: The layout of the in-house designed TPU chip exhibiting the ratio of the systolic array compared to the surrounding logic and controller.

TABLE I: Clock cycles required for Flex-TPU versus conventional TPU with static dataflow.

Model	Flex-TPU Cycles	Dataflow	Static Dataflow Cycles	Speedup
AlexNet [19]	8.598e+5	IS	1.176e+6	1.368
		OS	8.852e+5	1.030
		WS	1.188e+6	1.382
FasterRCNN [20]	3.922e+6	IS	5.640e+6	1.438
		OS	4.368e+6	1.114
		WS	4.710e+6	1.201
GoogleNet [21]	1.566e+6	IS	2.525e+6	1.612
		OS	1.660e+6	1.060
		WS	1.988e+6	1.269
MobileNet [22]	1.206e+6	IS	2.349e+6	1.949
		OS	1.373e+6	1.139
		WS	1.531e+6	1.270
ResNet-18 [16]	1.636e+6	IS	2.839e+6	1.736
		OS	1.718e+6	1.051
		WS	2.520e+6	1.540
VGG-13 [23]	2.172e+7	IS	2.971e+7	1.368
		OS	2.231e+7	1.027
		WS	3.046e+7	1.402
YOLO-Tiny [24]	2.131e+6	IS	3.729e+6	1.750
		OS	2.550e+6	1.196
		WS	3.337e+6	1.566

TABLE II: Area, power, and critical path delay overheads comparing the Flex-TPU to a conventional TPU with OS dataflow.

S	Area (mm^2)			Power (mW)			Critical Path Delay (ns)		
	TPU	Flex-TPU	Overhead	TPU	Flex-TPU	Overhead	TPU	Flex-TPU	Overhead
8×8	0.070	0.080	13.607%	3.491	3.756	7.591%	5.80	5.92	2.07%
16×16	0.284	0.318	12.180%	13.850	15.241	10.045%	6.44	6.48	0.62%
32×32	1.192	1.311	10.052%	55.621	61.545	10.650%	6.63	6.69	0.90%

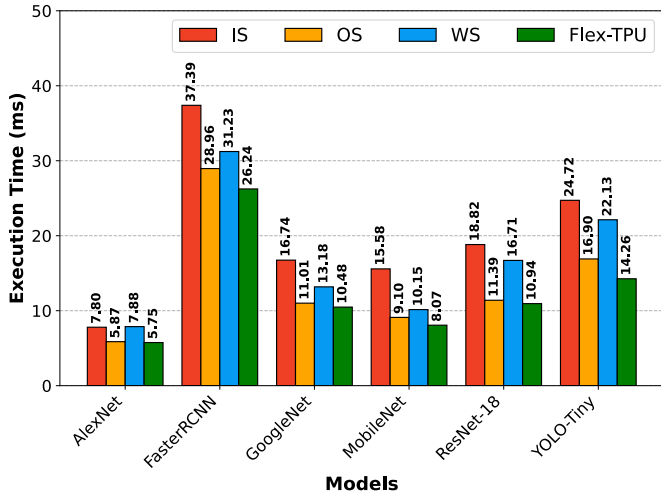


Fig. 6: The inference time per model for a systolic array size of $S = 32 \times 32$ for the varying dataflows: IS, OS, WS, and our Flex-TPU. VGG is not shown because its notably longer execution time disrupts the clarity of the graph.

array simulator [17], [18]. ScaleSim provides a layer-by-layer summary of the clock cycles required by a user-defined systolic array of size $S = N \times N$ to perform the inference computations of a specific DNN. Each of these DNNs is comprised of multiple convolutions and fully connected layers and is deployed on a TPU with $S = 32 \times 32$ systolic array. Table I, provides the total number of clock cycles required by each model using our Flex-TPU design as well as on a conventional TPU with a single static dataflow. As shown in Table I, the Flex-TPU provides a speedup of $1.027 \times$ to $1.949 \times$ across all models and dataflows.

Analyzing the speedup for each dataflow, most of the models perform close to optimally employing the OS dataflow compared to the IS and WS dataflows. Across the investigated models, the FasterRCNN and YOLO-Tiny appear to experience a greater speedup using the OS dataflow. On average, the Flex-TPU’s reconfigurable dataflow provides a speedup of $1.612 \times$, $1.090 \times$, and $1.400 \times$ compared to the single static dataflows of IS, OS, and WS, respectively. This implies that the IS and WS dataflows performed the poorest in terms of their overall computational execution time.

To determine the real-world execution time of each model running on a single dataflow, the number of clock cycles for each model was multiplied by the critical path delay of $6.63 ns$ for the conventional $S = 32 \times 32$ TPU. For the same $S = 32 \times 32$ size configuration of the Flex-TPU, we multiplied the optimal number of clock cycles found per layer by the Flex-TPU’s critical path delay of $6.69 ns$ to obtain each model’s

execution time. The execution times across the tested modes for both the static dataflows and the Flex-TPU are shown in Fig. 6. Across all models, the Flex-TPU is the best architecture in terms of execution time, outperforming conventional TPU architecture with static dataflows by as much as $10.99 ms$ which could be the determining factor of whether a model is considered real-time or not.

B. Power and Area Overheads

To examine the area and power utilization of our Flex-TPU architecture, we employ the Synopsys Design Compiler to synthesize a conventional TPU design along with the Flex-TPU under the same design constraints. These constraints consist of an uncertainty of 2%, a clock period of $10 ns$, and a clock network delay of $1 ns$. In particular, we synthesized three systolic array sizes consisting of $S = 8 \times 8$, 16×16 , and 32×32 for both the conventional TPU and our proposed Flex-TPU and report the area, power, and critical path delay for each in Table II. In this context, we focus solely on the OS dataflow architecture for the conventional TPU, as it achieves the best performance when compared to the IS and WS dataflow, as discussed in the previous subsection.

As expected, in Table II, the area and power consumption of the Flex-TPU are marginally higher compared to that of the conventional TPU with an overhead of at most 13.607% and 6.44%, respectively. Considering the potential average speedup of 36.7% achieved across all dataflows from Table I and the improved execution times shown in Figure 6, this area and power overhead could be considered acceptable depending on the network to be deployed and considering applications where the utmost speed is desired in a system.

While both the area and power increase in the Flex-TPU, the critical path delay remains very similar across each of the systolic array sizes (S), not exceeding more than 2.07% in the worst-case, i.e. $S = 8 \times 8$. This implies that the Flex-TPU’s architecture, if implemented in silicon, could have a very comparable clock frequency to the conventional TPU and further highlights the aforementioned speedups discussed as net speed increases in the Flex-TPU’s overall performance.

C. Scalability

Thus far, our Flex-TPU architecture results have consisted of small systolic array sizes of $S = 8 \times 8$, 16×16 , and 32×32 . These systolic array sizes would typically be used in smaller devices such as the Google Coral Edge TPU [25] since they are tailored for applications at the edge. In this subsection, we focus on investigating the current data center scale TPUs like the Google TPU v1 [3] with a 256×256 systolic array.

In Figure 7, we compare the TPU designs with static dataflow against our Flex-TPU architecture at a larger systolic

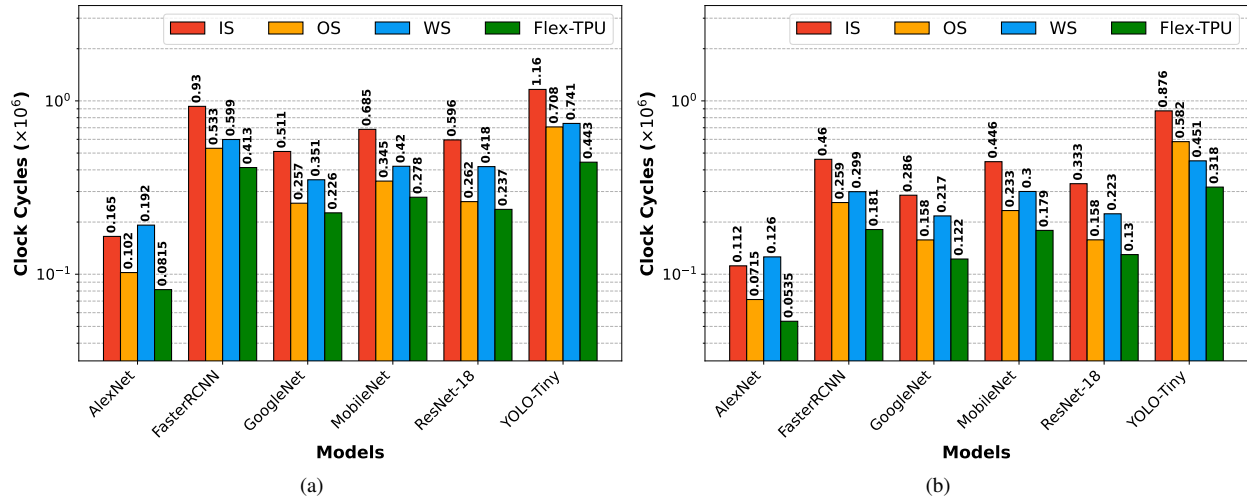


Fig. 7: The inference clock cycles per model for a systolic array sizes of (a) $S = 128 \times 128$ and (b) $S = 256 \times 256$ for the varying dataflows: IS, OS, WS, and our Flex-TPU demonstrating the scalability of our proposed Flex-TPU architecture.

array size of $S = 128 \times 128$ and 256×256 . Similar to the smaller scale $S = 32 \times 32$ systolic array, the Flex-TPU still provides a significant speed advantage compared to the IS and WS dataflow. However, compared to the TPU with OS dataflow, the Flex-TPU achieves further performance gains at scale. In particular, the Flex-TPU with the 128×128 systolic array achieves an average speedup of $1.238\times$, and the 256×256 achieves a $1.349\times$ speedup compared to the $1.090\times$ speedup of the 32×32 systolic array. This demonstrates the Flex-TPU’s effectiveness in further accelerating ML workloads in data centers at a larger scale.

IV. CONCLUSION

As AI and ML gain increasing traction in daily life, there is a rising demand for more performant systems and architectures for accelerating these workloads. While conventional TPUs have been instrumental in keeping up with this demand, their current static dataflow implementation potentially inhibits their full potential on some workloads. Thus, selecting an optimal dataflow specific to the workload can lead to significant performance gains. Herein, we proposed the Flex-TPU architecture highlighting the potential to further optimize the TPU design’s performance without limitations caused by static dataflows. The Flex-TPU accomplishes a runtime-reconfigurable dataflow by adding two multiplexers and a single register to each processing element. The experiments and simulation results demonstrate performance increases across various ML workloads with up to a $2.75\times$ speedup without incurring significant area and power overheads. Considering the popularity of current TPU accelerators in data centers and edge applications, the higher performance achieved by the Flex-TPU positions it as an appealing upgrade for future implementations of TPUs.

ACKNOWLEDGMENT

This work is supported by the National Science Foundation (NSF) under grant number 2340249.

REFERENCES

- [1] H. T. Kung and C. E. Leiserson, “Systolic arrays (for vlsi),” in *Sparse Matrix Proceedings 1978*, vol. 1. Society for industrial and applied mathematics Philadelphia, PA, USA, 1979, pp. 256–282.
- [2] N. Jouppi, “Quantifying the performance of the tpu, our first machine learning chip,” *Google Cloud Platform Blog*, Google, vol. 5, 2017.
- [3] N. P. Jouppi, C. Young, N. Patil, D. Patterson, G. Agrawal *et al.*, “In-datacenter performance analysis of a tensor processing unit,” in *Proc. of the 44th Annual Int. Symp. on Comput. Architecture*, 2017, pp. 1–12.
- [4] N. Jouppi, G. Kurian, S. Li, P. Ma, R. Nagarajan *et al.*, “Tpu v4: An optically reconfigurable supercomputer for machine learning with hardware support for embeddings,” in *Proceedings of the 50th Annual International Symposium on Computer Architecture*, 2023, pp. 1–12.
- [5] B. C. Reidy, M. Mohammadi, M. E. Elbity, and R. Zand, “Efficient deployment of transformer models on edge tpu accelerators: A real system evaluation,” in *Architecture and System Support for Transformer Models (ASSYST ISCA)*, 2023.
- [6] —, “Work in progress: Real-time transformer inference on edge ai accelerators,” in *2023 IEEE 29th Real-Time and Embedded Technology and Applications Symposium (RTAS)*, 2023, pp. 341–344.
- [7] H. Smith, J. Seekings, M. Mohammadi, and R. Zand, “Realtime facial expression recognition: Neuromorphic hardware vs. edge ai accelerators,” in *2023 International Conference on Machine Learning and Applications (ICMLA)*, 2023, pp. 1547–1552.
- [8] M. Mohammadi, H. Smith, L. Khan, and R. Zand, “Facial expression recognition at the edge: Cpu vs gpu vs vpu vs tpu,” in *Proceedings of the Great Lakes Symposium on VLSI 2023*, ser. GLSVLSI ’23. New York, NY, USA: Association for Computing Machinery, 2023, p. 243–248.
- [9] Google. Coral AI, “Tensorflow models on the edge tpu,” 2020. [Online]. Available: <https://coral.ai/docs/edgetpu/models-intro/#compatibility-overview>
- [10] Z. Wang, G. Wang, H. Jiang, N. Xu, and G. He, “Cosa:co-operative systolic arrays for multi-head attention mechanism in neural network using hybrid data reuse and fusion methodologies,” in *2023 60th ACM/IEEE Design Automation Conference (DAC)*, 2023, pp. 1–6.
- [11] M. E. Elbity, P. S. Chandarana, B. Reidy, J. K. Eshraghian, and R. Zand, “Aptpu: Approximate computing based tensor processing unit,” *IEEE Transactions on Circuits and Systems I: Regular Papers*, pp. 1–0, 2022.
- [12] P. Pandey, N. D. Gundi, K. Chakraborty, and S. Roy, “Uptpu: Improving energy efficiency of a tensor processing unit through underutilization based power-gating,” in *2021 58th ACM/IEEE Design Automation Conference (DAC)*. IEEE, 2021, pp. 325–330.
- [13] K.-C. Hsu and H.-W. Tseng, “Accelerating applications using edge tensor processing units,” in *Proceedings of the International Conference for High Performance Computing, Networking, Storage and Analysis*, 2021, pp. 1–14.

- [14] M. E. Elbity, B. Reidy, M. H. Amin, and R. Zand, "Heterogeneous integration of in-memory analog computing architectures with tensor processing units," in *Proceedings of the Great Lakes Symposium on VLSI 2023*, ser. GLSVLSI '23. New York, NY, USA: Association for Computing Machinery, 2023, p. 607–612.
- [15] K. Seshadri, B. Akin, J. Laudon, R. Narayanaswami, and A. Yazdanbakhsh, "An evaluation of edge tpu accelerators for convolutional neural networks," in *2022 IEEE International Symposium on Workload Characterization (IISWC)*, 2022, pp. 79–91.
- [16] K. He, X. Zhang, S. Ren, and J. Sun, "Deep residual learning for image recognition," 2015.
- [17] A. Samajdar, Y. Zhu, P. Whatmough, M. Mattina, and T. Krishna, "Scale-sim: Systolic cnn accelerator simulator," *arXiv preprint arXiv:1811.02883*, 2018.
- [18] A. Samajdar, J. M. Joseph, Y. Zhu, P. Whatmough, M. Mattina *et al.*, "A systematic methodology for characterizing scalability of dnn accelerators using scale-sim," in *2020 IEEE International Symposium on Performance Analysis of Systems and Software (ISPASS)*. IEEE, 2020, pp. 58–68.
- [19] A. Krizhevsky, I. Sutskever, and G. E. Hinton, "Imagenet classification with deep convolutional neural networks," in *Advances in Neural Information Processing Systems*, F. Pereira, C. Burges, L. Bottou, and K. Weinberger, Eds., vol. 25. Curran Associates, Inc., 2012.
- [20] S. Ren, K. He, R. Girshick, and J. Sun, "Faster r-cnn: Towards real-time object detection with region proposal networks," 2016.
- [21] C. Szegedy, W. Liu, Y. Jia, P. Sermanet, S. Reed *et al.*, "Going deeper with convolutions," 2014.
- [22] A. G. Howard, M. Zhu, B. Chen, D. Kalenichenko, W. Wang *et al.*, "Mobilenets: Efficient convolutional neural networks for mobile vision applications," 2017.
- [23] K. Simonyan and A. Zisserman, "Very deep convolutional networks for large-scale image recognition," 2015.
- [24] A. Bochkovskiy, C.-Y. Wang, and H.-Y. M. Liao, "Yolov4: Optimal speed and accuracy of object detection," 2020.
- [25] Google. Coral AI, "Edge tpu inferencing overview," 2020. [Online]. Available: <https://coral.ai/docs/edgetpu/inference/>